Open Source Evaluation of Power Transients Generated to Improve Performance Coefficient of Resistive Heating Systems

R.A Ainslie, H.W Gramm, G.A Lettenmaier, A.Palise, A. Gardiner, D Martin, S. Windisch

***Abstract*— The objectives of these tests are to replicate and evaluate the published heat signatures developed with an inductive resistive load. This is seen to require an aperiodic resonating frequency with subharmonics that are induced through the fine tuning of the interactive duty cycle of a MOSFET switching circuit. Results indicate that the produced transients enable improvements of performance efficiency well above COP 4.0 in line with the predictions of an alternative magnetic field model.**

***Index Terms*— Transient analysis, Heating, MOSFET circuits, Resistive circuits**

I. INTRODUCTION

The following tests were designed to replicate an experiment that was described in Quantum Magazine (Quantum Test) published in October, 2002. [1] That earlier test pointed to anomalous heat signatures that were achieved as predicted by a non classical magnetic field model, hereafter referred to as 'MMRA' (Magnetic Model by Rosemary Ainslie) [2]. This open source submission details the experimental apparatus, the applied measurements protocol and the data together with a variety of related tests that were designed to evaluate the adequacy of those applied test parameters. Because test replication results were in line with those detailed in the publication, it was considered that this submission of the experimental results would allow a wide dissemination both of the experiment and of the questions relating to those anomalies, as being preferred and required.

The classical approach to current flow recognizes that charge motion is predominately that of electric charge. The aspect of MMRA which is considered appropriate to this submission relates to current flow. It proposes that current flow comprises the motion of magnetic charge which, in turn comprises elementary magnetic dipolar particles. In classical terms, these particles would align with Faraday's Lines of Force and therefore the number of lines that exist through a particular real or imaginary surface, would still be represented as magnetic flux while the particles themselves, in distribution along those lines, represent the magnetic field.

These fields are extraneous to the atomic structure of matter and are thought to play a critical part in binding atoms and molecules into gross identifiable matter. Further, the particles obey an immutable imperative to move towards a condition of balance or zero net magnetic charge. Given a source material with an ionized charge imbalance which is measured as a potential difference, and given a closed circuit electromagnetic material path, these particles will return to the source material with the necessary charge to neutralize the imbalance.

Typical electronic circuits provide such material paths through the circuit components of which they are made which includes all conductors. During the passage of current flow through such closed circuitry it is proposed that the charge imbalance is transferred to those circuit components. The individual imbalances in each component and each conductor then seek balance according to that immutable imperative. In typical electronic circuitry, each component which has been 'charged' by this transfer, will either neutralize the charge internally, or influence a secondary current flow in anti-phase or opposite polarity to the first cycle.

While this is substantially in line with classical assumption as it relates to the transfer of charge, the distinction is drawn that the energy that is then transferred to such electromagnetic components, is able to regenerate a

Manuscript received Dec 1, 2009. This work was supported entirely as a global open source project by independent persons oriented toward its success. The entire financial burden has rested on individual participants and their willingness to share resources as needed toward the success of this work.

R. A. Ainslie (e-mail: ainslie@mweb.co.za)

H. W. Gramm is with Universal Research And Development of Baldwin Park, CA 91706 USA (e-mail: hgramm@urad.net)

secondary cycle of current flow in line with electromagnetic laws. This energy is then not limited to the quotient of stored energy delivered during the first cycle and as presumed by classical theory. Instead it is dependent on the circuit component's material characteristics and the means by which those materials balance a charge put upon them. Therefore there is a real energy potential in the secondary cycle which would reflect in a measured improvement to the performance coefficient of the circuit arrangement. This improvement may be at the expense of the material bonds. In a worst case condition, this energy may be released as is observed in an exploding wire that is put under extreme charge conditions due to excessive current flow. In a best case condition, the energy is released gradually over time and is added to the natural energy conversions employed by the circuit. This paper addresses an application of the MMRA and a demonstration of such a gradual release.

The circuit was designed with a switch to enable this secondary cycle of current flow. It was found that the performance co-efficient was enhanced through an applied duty cycle that allowed the circuit to generate its preferred mode of oscillation. This was seen to require an aperiodic, self-regulated resonating frequency with a distinctive harmonic associated with that enhanced performance. However the precise parameters of the duty cycle, determined by adjustment of the potentiometer at the gate [8] of the metal-oxide-semiconductor field-effect transistor (MOSFET), were found to be both critical and elusive. The fact that these benefits to an enhanced co-efficient may have been overlooked, could be attributed to the narrowness of the range required for this setting. Under usual applications such aperiodicity is considered undesirable and therefore systematically factored out of standard switched applications.

A series of related tests included evaluation of the inductance required on the load resistor to optimize the effect, as well as an evaluation of the comparative diameters of that resistor to explore optimized conditions. Other tests and measurements were performed to address a variety of concerns including grounding issues, any possible breach of Kirchhoff's Current Law, voltage differentials and applied high frequencies without the required harmonics.

Test results appear to be consistent with the results in the published test but the actual measurements indicated a potential for an absolute conservation of charge at the supply. The conclusions to the tests include a broad discussion of the constraints to measurements and indicate a need for expert evaluation of both the results and the theoretical paradigms that predicted the results.

II. Experiment

A. Description

The experiment described herein is one example taken from more than 14 individual tests that were considered to demonstrate a performance improvement. All of the tests demonstrate various aspects of the preferred operation as well as exposing specific characteristics peculiar to the circuit being evaluated. It can be observed in the available test data that progressive development toward performance improvements and refinement of the measurement, are evident.

The positive terminal of a 24 volt battery bank is applied in series with a 10 Ohm wire wound inductive resistive load, an N-Channel Power MOSFET (Q1) Fig. 1 and a 0.25 Ohm shunt resistor (R2) Fig. 1. A separate 12 volt battery supplies a 555 (U1) Fig. 1 switching circuit which is capable of variable duty cycles and frequency adjustments. Q1 was chosen with an avalanche protection body diode [7] feature that enables conventional reverse current flow during the off period of the duty cycle and protects against high voltage counter electromotive force (CEMF).

U1 drives the gate of Q1 directly through a precision variable resistor (R1) Fig. 1. Specific adjustment of R1 and the variable resistors R4, and R7 shown in Fig. 1 enables a preferred mode of oscillation that overrides the predetermined frequency and duty cycle. The fundamental and harmonic waveforms that result vary greatly from one cycle to another. The transient voltages that are deliberately generated, then compound this variation. The duty cycle is adjusted using R4 and R7 whereas R1 is critical in enabling the preferred self oscillation.

B. Equipment and Connections

A Tektronix TDS3054C Digital Phosphor Oscilloscope (DPO) [5] was provided to us offering 500MHz bandwidth; digital storage capability and the ability to data capture 10K records at any one time period. We used 4 probes as outlined in Fig. 2 and detailed in section D herein. We also used a Fluke 87 True-RMS DMM [6] across the 24V battery bank as a visual guide during the tuning process. A Fluke 62 Mini Infrared Thermometer [10] was used for all temperature measurements and was held at the distance needed to ensure proper readings without background interference. For example, the 32mm load resistor required a measurement distance of no more than 320mm to ensure the reception area remained within the diameter (girth) of the resistor according to the spot ratio of 10:1. The

ambient temperature was always measured at least one meter from the components radiating thermal energy.

C. Preferred mode of oscillation

Establishing the preferred mode of oscillation involves several interactive readings and a trained eye in order to get things aligned properly. Because the nature of the aperiodic operation involves a self resonance which results in retriggering U1 (see Fig. 1.) the preferred mode of oscillation ignores the timing functions which are initially set to begin oscillation. There is a known interaction between U1 and Q1 that make this possible, however, it is believed by this author that this effect could be synthesized once the predominate sweep frequency and specific subharmonics are accurately identified. Determining those characteristics was beyond the scope of this endeavor. The procedure toward obtaining the preferred mode of oscillation is relatively straightforward but somewhat arduous and requires a developed skill. While monitoring the four waveforms on the oscilloscope [5] the voltage across the shunt was monitored on Channel one (CH1) and the mean value was displayed in the right margin. Adjustments are made on R1 (see Fig. 1.) to produce the lowest mean value while monitoring the 24V battery voltage with the Fluke [6]. When the circuit is operating outside the desired parameters the battery voltage drops noticeably due to the power drain. The adjustment is sought that causes a stabilization or slight increase in battery voltage. It has been determined that there is an observable delay between the signal from U1 to turn off Q1 and the inductive collapse of the magnetic field associated with the load resistor R3; this is desirable and necessary to produce the preferred mode of oscillation. In our tests this delay was typically around 350ns. The inductive collapse of the magnetic field associated with R3 was monitored on Channel two (CH2) as a voltage increase at the drain pin of Q1. The drive signal was monitored on Channel three (CH3) as the voltage measured on pin 3 of U1. The time between the falling edge of CH3 and the rising edge of CH2 is the delay being discussed. An additional parameter that is not critical but preferred is good amplitude on the CH2 signal. When all four of these conditions are found the circuit is in the preferred mode of oscillation offering an improved performance. As one might imagine, tuning this mode with a single adjustment is no easy task because of the interactive and recursive nature of the aperiodic frequencies.

D. Data Analysis

In evaluating the data obtained at regular intervals we observed that our resolution was greater at the faster time base but this was at the expense of the quantity of cycles required for a good average. The oscilloscope [5] vertical settings were set for voltage inputs while the horizontal settings were set to the desired time base. Using the 2V/div vertical scale with 40µs/div horizontal provided two decimal places or 10mv resolution and with 2µs/div provided six decimal places of resolution or 1µV. Similarly, using the 100V/div setting provided us with integer values or 1V resolution in the 40µs/div setting, and four decimal places or 100 µV in the 2µs/div setting. In the preferred mode of operation a typical 20µs period, that is one full screen capture at 2µs/div, would capture approximately 6 to 10 complete cycles. The oscilloscope provided excellent sample resolution of 10k samples per screen capture and this ensured accurate data collection for the frequencies observed. The entire spectrum is aperiodic in the preferred mode of operation with a fundamental frequency usually near 3.5 kHz but ranging from 140 kHz to above 500 kHz and various subharmonics which are observed to modulate the amplitude of the fundamental in superposition [3]. It was determined that approximately 140µs of data would contain about six intervals of the superimposed signal and therefore the 400µs captures of 40µs/div would be sufficient to provide a good average of operation. Analysis was performed for each individual capture as well as an average of the composite of each 40µs/div and 2µs/div. The data captures at each six minute interval during the one hour test were taken in that order with just a few seconds in between each capture limited only by the physical need to set the oscilloscope to the desired horizontal time base setting as the scripting features were not used for this process.

The data comprises the capture of four channels of voltage measurements and a relative time marker. The associated points of measurement can be seen in Fig 2 as follows: Channel one (CH1), the yellow probe is the instantaneous voltage measured across R2 at the junction of R2 and the 19mm (0.75in) bare wire connection to the source pin of Q1. Channel two (CH2), the blue probe is the instantaneous voltage measured at the drain pin of Q1. Channel three (CH3), the magenta probe is the instantaneous voltage measured at the timer NE555-PIN 3. Channel four (CH4), the green probe is the instantaneous voltage measured at the Voltage Source Measurement Location on the Positive Feed Wire (See Fig. 2). The objective of the analysis was to determine the average source power delivered to the load so as to compare that value to the required baseline for the same relative temperature of the load. In this way it could be determined if the circuit is providing an improvement when compared to the standard DC power baseline.

The data imported into the spreadsheets represented columns A - E for Time Marker, CH1, CH2, CH3 and CH4 respectively. A new column G was used for the power calculation using the spreadsheet formula E:x*(B:x/0.25)

where E and B are the column references, x is the row number and 0.25 represents the resistance of the shunt in ohms. This formula is copied to all rows in column G and represents the power formula P=EI where I is the instantaneous voltage of CH2 divided by the resistance of R2. A comparison was made between an average of all the rows of data for each column and just those rows which represented complete cycles with no significant difference. Also, an application of the Simpson's Rule [4] was made to determine if the parabolic treatment of the waveforms would offer any substantial difference as compared to the spreadsheet average function (2). The formula used relates to the composite Simpson's Rule in the form (1) where *n* is even and $\Delta x = (b - a)/n$.

$$\int_a^b f(x)dx \approx S_n = \frac{\Delta x}{3}\left[f(x_0) + 4f(x_1) + 2f(x_2) + 4f(x_3) + \cdots + 2f(x_{n-2}) + 4f(x_{n-1}) + f(x_n)\right] \quad (1)$$

The total number of data rows in the spreadsheet range from row 2 to row 10001, therefore only 9998 rows could be used for the approximate integration using the Simpson's Rule. The difference from the spreadsheet average function and the Simpson's Rule approximate integration was within 0.04W for 21 of the collections with the 22nd collection being 0.05W difference. Table II shows the source power average and Simpson's Rule Integration for each sheet from the test which consisted of 22 data dumps taken at 6 minute intervals over a one hour period. At each interval two data dumps were recorded; one for 40µs/div and one for 2µs/div. The time between a 40µs/div data dump and a 2µs data dump for any given interval is only a few seconds. The temperature recordings as they relate to each sheet are found in Fig. 3 and the baseline chart is found in Table III.

III. Measurements Protocol

A. Energy To and From the Battery Supply

Current flow to and from the battery was determined from the voltage waveform across the 0.25 Ohm non-inductive sense resistor (shunt) divided by its resistance. The use of that shunt minimizes the inaccuracies that relate to the measurement of impedance to an oscillating waveform. Typically, batteries are not able to deliver a negative current flow. Therefore, it was determined that current delivered by the battery would be the product of instantaneous voltage measured across the shunt divided by the resistance of the shunt measured above zero. Correspondingly, any current delivered back to the battery would be determined from the instantaneous voltage across the shunt divided by the shunt's resistance, measured below zero. The net flow of current from the battery would be the difference between these two values.

To ensure both positive and negative transitions were accurately recorded the oscilloscope was set to direct current (DC) coupling. Multiple data dumps of ten thousand samples each were stored and downloaded to spreadsheet for analysis. The equation applied in the analysis for source power determination was

$$\frac{\sum_{n=1}^{x} VI}{x} \quad (2)$$

where V is the source voltage where measured, I is the current calculated at the shunt and X is the number of samples analyzed.

B. Energy Dissipated at Load Resistor

The inductive property of the load resistor was required to generate high voltage spikes during the off period of each switching cycle. Also, the impedance varies with frequency and temperature which makes it difficult to determine the accurate instantaneous impedance of the load resistor at any given moment. These conditions caused protracted discussion on the accuracy of measurement related to current phase lag within the inductive component of the load. To address these concerns it was agreed to confine the measurement of power dissipated to caloric values as proof of dissipated energy.

Measurement of the load resistor temperature was enabled through the use of an Infra Red Thermometer chosen because it is not easily affected by electromagnetic interference. The readings were recorded from the digital display in degrees Fahrenheit and were conducted in a draft free environment. Ambient room temperature was recorded consecutively. Temperature measurements were also taken of R2 and Q1 and the results recorded as represented on the attached schedule. The difference between ambient room temperature and the load resistor was considered to represent the actual caloric value under test conditions.

The heat profile of the load resistor was manually calibrated using a variable power supply source. The supply was increased from 4.8 volts to 8.8 volts in increments of 0.2 volts each. At each interval the amperage was recorded and the power was then calculated as V*I. When stabilized after each interval the resistor temperature and the ambient temperature were recorded. The entire calibration was performed in a draft free environment. Table III shows the results of the calibration.

IV. Mesh Currents

This paper would not be complete without some discussion regarding the interactions between the timer circuit and the heating circuit. Each circuit has an independent supply source and it was necessary to consider whether the observed improvements could be attributed to a power exchange from the timer supply to the heating load. While a DC approach to this concern is relatively straight forward as there is a DC barrier between the Q1 gate and the other two circuit paths via the drain and source pins, we must consider that there is an AC path or Pulsed DC path through this barrier. The various capacitances and even the stored energy in the inductances of the leads in Q1 can work as charge carriers passing energy back and forth across that barrier. U1 can source and sink a maximum 200mA and has a maximum operating temperature of 70°C [11]. Since this is the only conductive path for current to flow in, these parameters limit how much power can be passed via this pathway. In addition, the 2800pF C_{iss} [12] of Q1 represents a capacitive reactance of around 160 ohms at the fundamental frequency. Also, we have a few ohms of resistance in R1 as part of the combined limit. Therefore if we conservatively calculate the resistance of R1 to be only 2 ohms and we discount any reactive impedance of the load resistor and take it at its resistive value of 10 Ohms giving us 12 Ohms to add to the 160 Ohm impedance caused by the capacitive reactance we arrive at a conservative resistance of 172 Ohms. Now if we were able to pass the maximum allowed current of 200mA through that resistance we would need 34.4V. Therefore, the maximum instantaneous power we could transfer through that path would be approximately 6.8W. So in order to answer the question as to whether this could in fact occur we deemed it necessary to perform an auxiliary test wherein we placed a second current sensing resistor in the interconnect path at the Voltage Source reference point. With the understanding that all of the current sourced by the timer circuit battery must return to that battery and the interconnect being the only path by which it could occur we felt that any power being transferred into the gate must then return via the interconnect wire. For this test we removed the probe from the U1 Pin 3 position and placed it on the secondary current sensing resistor lead connected to the interconnect wire identified in Fig 2 as a possible shared current path. The circuit was run in its preferred mode of operation and a data dump was performed using the 2µs/div time base. We were expecting some portion of the R3 charging current to be finding its way through that path in a parallel manner bypassing the R2 sensing resistor and fully expected the need to add this current to the existing current to get a full picture of the operation. To our surprise the net value of the current running in that leg was ***negative.*** Nevertheless an integration of both currents was necessary to get the real picture. The results indicate that a mesh current [9] flows through the source pin of Q1and actually inflates the current reading by a value of less than 1W which means the improvements we have documented are conservative by that quantity. As far as any currents being supplied by the timer circuit and flowing through the load resistor and 24V battery bank, that current would have been present in the same interconnect wire on its return path. Even if all the current found in this case was attributed to such an unlikely path it still falls short of the observed performance increases.

V. Overview Of Results On Tests 1-13

The following schedule lists the numbered tests conducted together with reference to the objective of each test. It provides a hyperlink to the original data for precise detailed reference. This method of presentation was preferred in line with the principles of open source allowing access to the data.

Test 1
This test was conducted on a standard commercial resistor (Stock, R3S) of 10 Ohm. No gains were evident.
http://www.energeticforum.com/renewable-energy/4314-cop-17-heater-rosemary-ainslie-96.html#post69858

Test 2
Load resistor specially manufactured (Custom, R3C) to assessed Quantum test specifications. No gains were evident.
http://www.energeticforum.com/renewable-energy/4314-cop-17-heater-rosemary-ainslie-97.html#post69966

Test 3
R3C used. First gains evident but records only partially completed test. First evidence of the required harmonic.
http://www.energeticforum.com/renewable-energy/4314-cop-17-heater-rosemary-ainslie-97.html#post69966

Test 4
R3C used. No gains evident and also the loss of the required harmonic.
http://www.energeticforum.com/renewable-energy/4314-cop-17-heater-rosemary-ainslie-99.html#post70432

Test 5
R3C used. Gains were evident together with evidence of the required harmonic.
http://www.energeticforum.com/renewable-energy/4314-cop-17-heater-rosemary-ainslie-99.html#post70771

Test 6
R3S used. No gains evident. Nor could the required signature harmonic be found.
http://www.energeticforum.com/renewable-energy/4314-cop-17-heater-rosemary-ainslie-99.html#post71062

Test 7
R3C used. Gains evident but actual power values exceeding the voltage constraints of the DPO. Test was terminated but does point to the feasibility of advantages at higher power output.
http://www.energeticforum.com/renewable-energy/4314-cop-17-heater-rosemary-ainslie-99.html#post71364

Test 8
R3C used. Circuit was now assessed as workable for the required effect. Therefore were alligator clips removed and all leads shortened and soldered. Gains were evident. Required harmonic was again evident.
http://www.energeticforum.com/renewable-energy/4314-cop-17-heater-rosemary-ainslie-104.html#post73814

Test 9
R3C used. Non-inductive precision shunt resistor replaced. Gains were evident.
http://www.energeticforum.com/renewable-energy/4314-cop-17-heater-rosemary-ainslie-105.html#post74402

Test 10
R3C used. Test 9 effectively re-run to improve on results. Gains were evident indicating no material difference in the voltage values between the inductive and non-inductive shunt.
http://www.energeticforum.com/renewable-energy/4314-cop-17-heater-rosemary-ainslie-105.html#post74402

Test 11
R3C used. This test was conducted over a one hour period with intensive sample capture to determine that the range of voltage across the shunt fell within acceptable levels.
http://www.energeticforum.com/renewable-energy/4314-cop-17-heater-rosemary-ainslie-105.html#post74402

Test 12
New resistor wound as a further attempt to duplicate the properties of the original Quantum Test. No gain observed and evident loss of the required harmonic.
http://www.energeticforum.com/renewable-energy/4314-cop-17-heater-rosemary-ainslie-105.html#post74402

Test 13
R3C Used This is the sample test.
http://www.energeticforum.com/renewable-energy/4314-cop-17-heater-rosemary-ainslie-105.html#post3177

VI. Discussion

As the objective of the test is to evaluate the advantages in generating that second cycle from a switching circuit, a battery supply source was used. It is understood that a battery cannot deliver energy in open circuit conditions and

any energy evident to the circuit during the off period would therefore be sourced away from that supply. What was evident in the voltage waveform, as measured at the source, was that the spike at the drain was able to recharge the battery. This spike results from the collapsing fields in the inductive load resistor. The extent of that recharge was also evident in the reading of a voltmeter placed directly across the battery terminals.

As battery performance requires separate and specific evaluation disciplines, it was considered to be outside the scope of this submission and those records of duration and voltage levels were simply included as a reference. However actual test results indicated a net loss to the battery voltage notwithstanding the evidence of zero net loss in some measurements. This is variously attributed to inductance in the wire that may have distorted measurements or to occasional loss of the overlying harmonic during circuit operation, which loss is seen to diminish efficiency.

Replication of the original circuit conditions as these relate to applied frequency and duty cycle were not successful. But there is evidence that the publication included erroneous data in the details of the resistor winding which necessitated a best guess approximation in the choice and manufacture of the resistor apparatus used for these tests.

Also of concern was that the point of our Source Power reference ground used for the probes and timer interconnect point was positioned about 15cm away from the shunt with an apparent effect as that of a 100nH inductor which increased the overall amplitude of the shunt voltage measurements of tests 1 through 10. Measurements of test 11 onwards included the repositioning of this reference point directly onto the shunt lead. Interestingly, this did reduce the overall amplitude of that measured signal which required the vertical setting on the oscilloscope to be reduced to 1V/div; however the net mean voltage reading actually dropped indicating a greater improvement in performance.

Tests 1 through 8 included the use of a wire wound shunt with some inductance associated with that winding. To obviate this, all tests recorded inclusive of test 9 onward were done with a replacement non-inductive shunt as detailed in the Components schedule. But there was very little evidence of difference and the indications are that those measurements taken in the first tests were not seriously impacted by the inductance of the early shunt.

Of interest is the fact that the circuit was able to run for extended periods at less than half the optimum charged condition of the battery while still dissipating energy at the load resistor. The indications here were that the resonating condition of the supply and the inductive components of the resistor were able to sustain a potential difference to enable a continual exchange. This test is only referenced to encourage further investigation of this effect. Any test results which may appear to relate to battery performance are not detailed as battery performance analysis is considered to be outside the scope of this replication exercise.

Most tests indicated a marginal net loss to the voltage of the source batteries notwithstanding periods of an evident recharge. This is in line with results in the Quantum Test. This loss is variously attributed to the momentary and occasional loss of the signature harmonic that is required for optimization of results. But the evidence is that, subject to the sustainability of that harmonic, the theoretical indications are that battery discharge can be obviated. This directs attention to the need for some manufactured means of sustaining that harmonic that may be required in optimized conditions of application and, in turn, requires further research.

Apart from the anomalous heat signatures developed over the resistive load is the evidence of anomalous waveforms that point to the simultaneous and alternate current paths that can be developed across a circuit. These results raise some questions as they relate to Kirchhoff’s Laws and further emphasize the proposal that some alternate principle may need to be incorporated into known paradigms to account for these effects. Of interest is that the waveforms are replicable in simulated programs, e.g. Spice and suggests that classical algorithms can account for the classical electromagnetic interactions, however phase shifts in current were not easily modeled and the reality suggests a unique complex arrangement that manifests as an improvement in performance.

VII. Conclusion

The Quantum Test results were substantially replicated. While the performance coefficient was not as high in the test chosen for description, there is evidence that more energy is in fact being returned to source than is measured across the shunt. This was shown in the measurement of current flow to the switching circuit referenced in the discussion. There was also evidence of zero net loss in the integration of measurements on tests 3, 5, and 7. These tests effectively outperformed the Quantum Test, pointing to development requirements to sustain this potential.

While these results may confront classical constraints as they relate to the transfer of energy, and as predicted in terms of the MMRA , it is hoped that the proposals in that field model may be considered or that mainstream explore alternate models to account for these effects. The evidence is that it is possible to partially or entirely conserve energy while developing anomalous heat signatures over resistive loads. This, in turn, points to the need to revise current applications to exploit this benefit which may then obviate some of the pollutant effects associated with energy generation.

It is hoped that this submission will encourage the required investigation and that this document may serve as a foundation to more systematic research into the study and development of these parameters.

ACKNOWLEDGEMENT

We as a collective group extend our heartfelt gratitude to Tektronix for the generous use of the required TDS3054C DPO.

Thanks to the varied and extensive contributions from open source members including A. Murakami, P. Lindemann, Dr Stiffler, L. Choquette, M.J . Nunnerley, C. Schjedahl, T. J. C. Gramm, J. R. Gramm.

Also with gratitude to those that prefer to remain anonymous including, suchyo, eternalightwithin, groundloop, Joit, elias, Lllabarre, Kenny_PMM.

And special thanks to those in that open source community who disputed the results for their varied and often constructive criticisms but who advised us that they do not want specific mention.

To those many academics who have asked to remain anonymous and who guided us in the test protocols and to the advice and interest expressed by many other experts who also prefer to remain anonymous.

REFERENCES

[1] R. A. Ainslie, B. C. Buckley, “Transient energy enhances energy co-efficients”, Quantum Magazine October 2002, pp. 5-8 Photocopy Available: (http://www.free-energy.ws/pdf/quantum_october_2002.pdf)

[2] R. A. Ainslie, D. Martin, “A UNIFYING FIELD MODEL”, unpublished, [online] Available: http://rosemaryainslie.blogspot.com/2008/09/test.html

[3] Edward J. Ross, *Professional Electrical/Electronic Engineer’s License Study Guide*, 1st ed. Blue Ridge Summit, PA: Tab Books, 1977, page 329

[4] James Stewart, *Calculus Early Transcendentals, 5th ed. Belmont, CA: Thomson Brooks/Cole, pp. 522 - 524*

[5] Tektronix TDS3054C 500 MHz 4 Channel Digital Phosphor Oscilloscope Data Sheet [online], Available: http://www2.tek.com/cmsreplive/psrep/13406/41W_12482_17_2009.07.16.16.00.09_13406_EN.pdf

[6] Fluke 87 True-RMS Multimeter User Manual [Online]. Available: http://assets.fluke.com/manuals/87_____umeng0800.pdf

[7] International Rectifier, *HEXFET Power MOSFET Designer’s Manual,* 2nd ed. vol. 3, El Segundo, CA: 1995, pp. 1575-1581

[8] International Rectifier, *HEXFET Power MOSFET Designer’s Manual,* 2nd ed. vol. 3, El Segundo, CA: 1995, pp. 1541-1566

[9] Edward J. Ross, *Professional Electrical/Electronic Engineer’s License Study Guide*, 1st ed. Blue Ridge Summit, PA: Tab Books, 1977, pp. 332-333

[10] Fluke 62 Mini Infrared Thermometer Information Site, [online] Available: http://us.fluke.com/usen/products/Fluke+62.htm

[11] *The Linear Control Circuits Data Book for Design Engineers,* Texas Instruments Incorporated, 2nd ed., 1980, pp. 282-283.

[12] International Rectifier, *HEXFET Power MOSFET Designer’s Manual,* 2nd ed. vol. 3, El Segundo, CA: 1995, page 1116

Table I – Circuit Components	
Part	Description
C1	0.01 µF Capacitor
C2	0.001 µF Capacitor
C3	0.047µF Capacitor
C4	100 µF Capacitor
D1	1N4007 Diode
D2	1N4148 Diode (1N914)
D3	1N4148 Diode (1N914)
Q1	IRFPG50 HEXFET MOSFET, International Rectifier
R1	100 Ohm Potentiometer 10-Turn 2-watt, Vishay Spectrol #SP534
R2	0.25 Ohm 30 watt 1% non-Inductive Resistor, Caddock Electronics Inc. #MP930
R3	10 Ohm + - 5% Prototype wire wound “Quantum” Load Resistor
R4	2K Ohm Potentiometer 10-Turn 2-watt, Vishay Spectrol #SP534
R5	110 Ohm 1/8 watt Resistor
R6	330 Ohm 1/8 watt Resistor
The specific manufacturers of circuit components are provided where known.	

Table II - Source Power Averages and Integration for test 13		
Sheet Number	AVG	SRI
TEK00000	0.00	0.01
TEK00001	-1.05	-1.06
TEK00002	3.60	3.61
TEK00003	3.98	4.00
TEK00004	2.96	2.93
TEK00005	5.59	5.58
TEK00006	-0.87	-0.89
TEK00007	-0.44	-0.40
TEK00008	0.39	0.39
TEK00009	-1.17	-1.12
TEK00010	4.92	4.88
TEK00011	-1.59	-1.55
TEK00012	-0.17	-0.20
TEK00013	-0.41	-0.41
TEK00014	0.09	0.10
TEK00015	5.12	5.15
TEK00016	-0.71	-0.71
TEK00017	2.39	2.39
TEK00018	-0.42	-0.44
TEK00019	0.13	0.15
TEK00020	-0.12	-0.13
TEK00021	6.45	6.40
AVERAGES	1.30	1.30

TABLE III
Table 3 – Schedule of Custom Load Resistor Temperature Baseline

VOLTS DC	AMPS	°F	AMBIENT	DIFFERENCE	WATTS
4.8	0.50	107	73.5	33.50	2.40
5.0	0.52	110	73.8	36.20	2.60
5.2	0.54	114	73.9	40.10	2.81
5.4	0.56	116	73.8	42.20	3.02
5.6	0.58	118	73.6	44.40	3.25
5.8	0.60	120	73.8	46.20	3.48
6.0	0.62	122	73.9	48.10	3.72
6.2	0.64	125	73.8	51.20	3.97
6.4	0.66	128	73.9	54.10	4.22
6.6	0.68	131	74.1	56.90	4.49
6.8	0.70	134	74.1	59.90	4.76
7.0	0.72	137	74.2	62.80	5.04
7.2	0.74	139	74.3	64.70	5.33
7.4	0.76	142	74.7	67.30	5.63
7.6	0.78	146	74.9	71.10	5.93
7.8	0.80	148	75.0	73.00	6.24
8.0	0.82	153	75.0	78.00	6.56
8.2	0.84	155	74.9	80.10	6.89
8.4	0.86	157	74.5	82.10	7.22
8.6	0.88	159	74.5	84.50	7.57
8.8	0.90	164	74.6	89.40	7.92

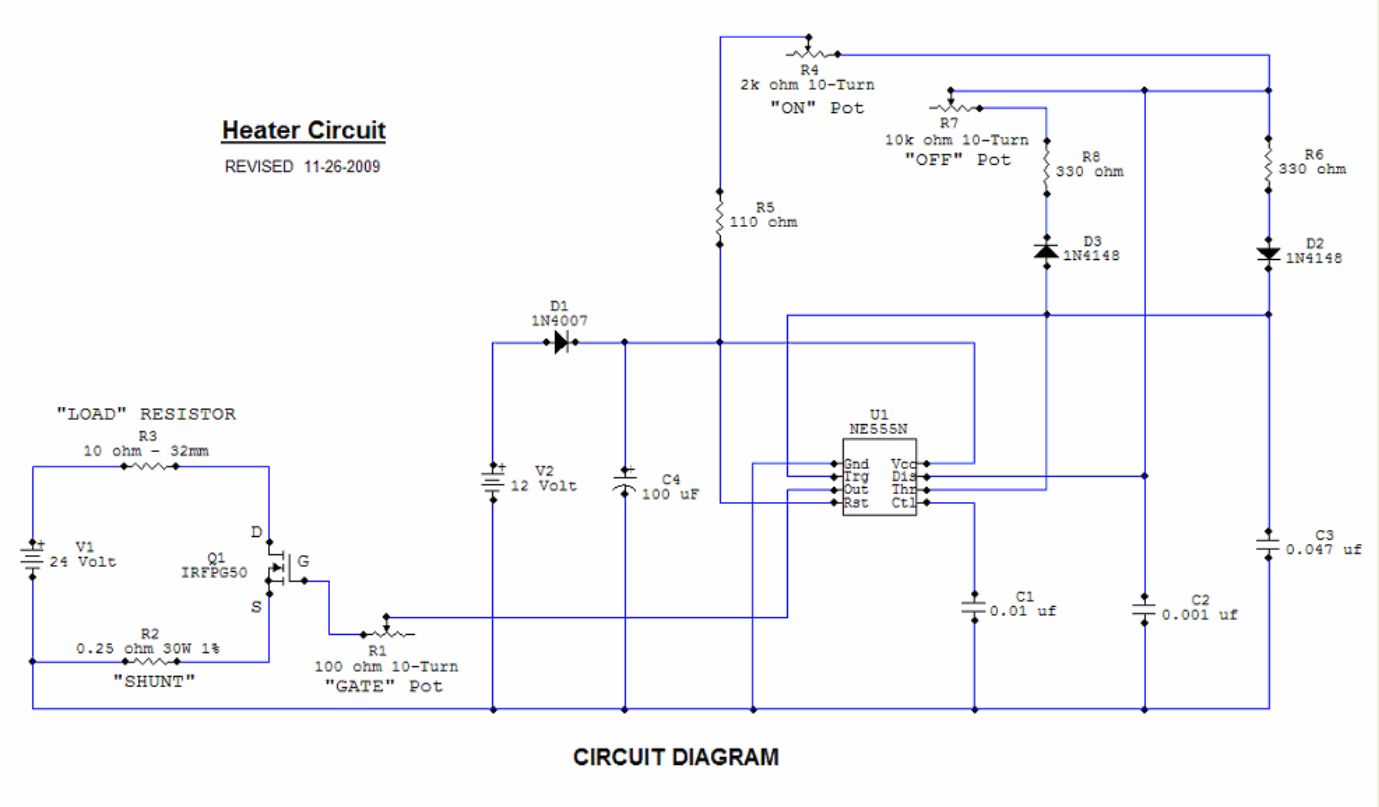

Fig. 1. MOSFET heating circuit

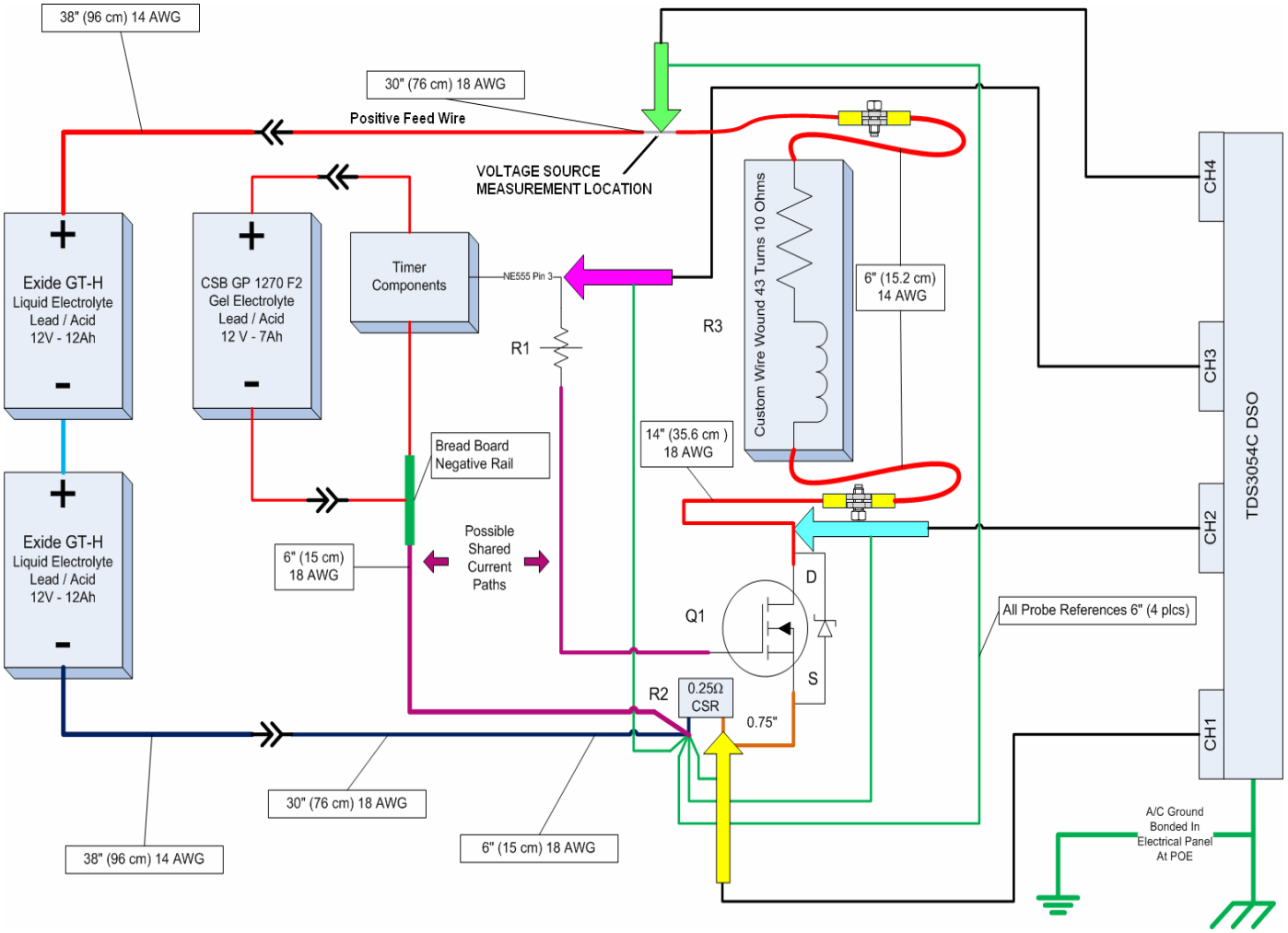

Fig. 2. Wiring Diagram showing probe locations and wire sizes.
Please note that the probes shown as colored arrows are color coded to the respective trace colors associated with test screen shots.

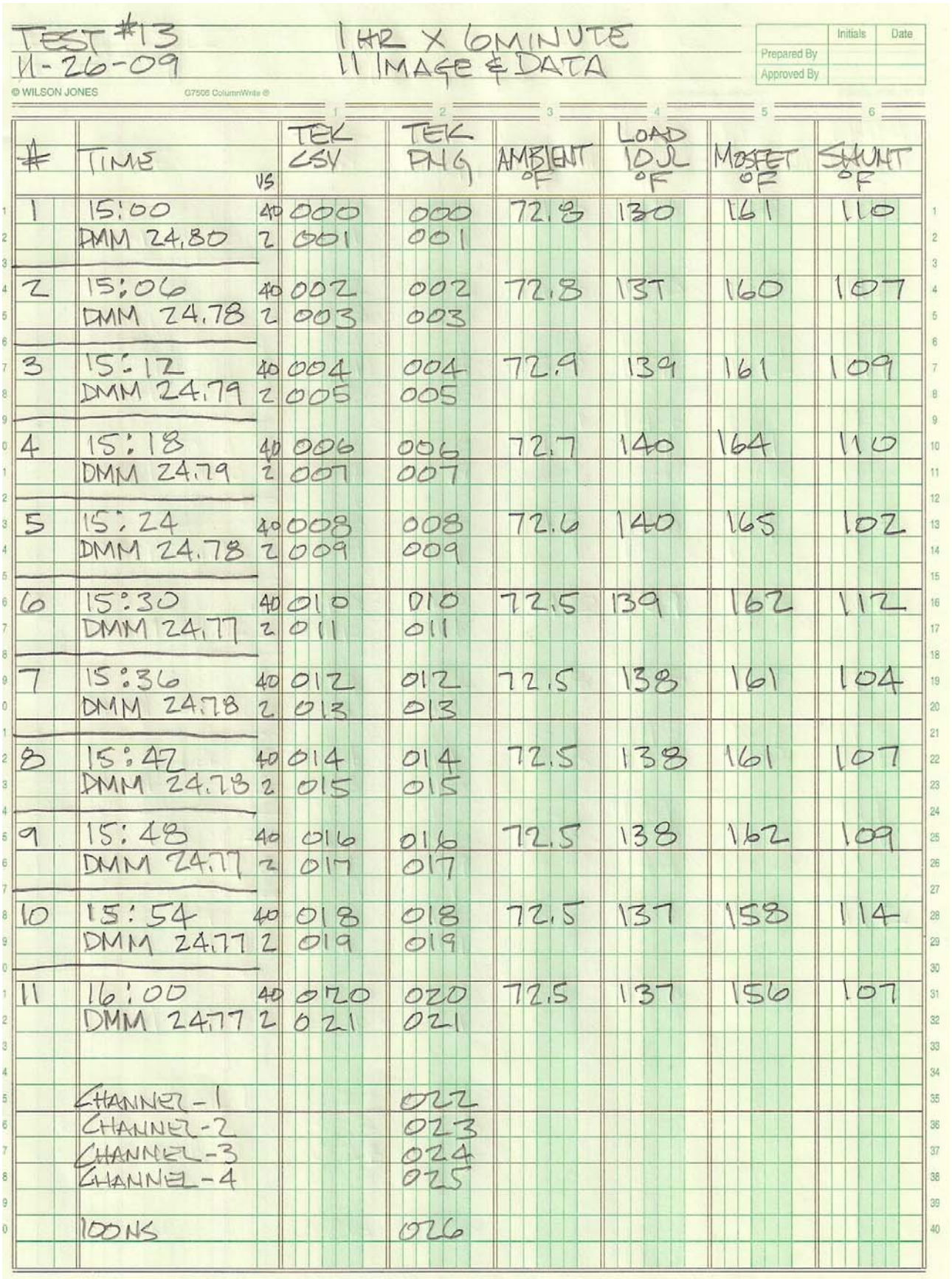

TEST #13 — 1 HR X 60 MINUTE
11-26-09 — 11 IMAGE & DATA

	Initials	Date
Prepared By		
Approved By		

© WILSON JONES G7506 ColumnWrite ®

#	TIME	VS	TEK CSV	TEK PNG	AMBIENT °F	LOAD IDLE °F	MOSFET °F	SHUNT °F
1	15:00	40	000	000	72.8	130	161	110
	DMM 24.80	2	001	001				
2	15:06	40	002	002	72.8	137	160	107
	DMM 24.78	2	003	003				
3	15:12	40	004	004	72.9	139	161	109
	DMM 24.79	2	005	005				
4	15:18	40	006	006	72.7	140	164	110
	DMM 24.79	2	007	007				
5	15:24	40	008	008	72.6	140	165	102
	DMM 24.78	2	009	009				
6	15:30	40	010	010	72.5	139	162	112
	DMM 24.77	2	011	011				
7	15:36	40	012	012	72.5	138	161	104
	DMM 24.78	2	013	013				
8	15:47	40	014	014	72.5	138	161	107
	DMM 24.78	2	015	015				
9	15:48	40	016	016	72.5	138	162	109
	DMM 24.77	2	017	017				
10	15:54	40	018	018	72.5	137	158	114
	DMM 24.77	2	019	019				
11	16:00	40	020	020	72.5	137	156	107
	DMM 24.77	2	021	021				
	CHANNEL-1			022				
	CHANNEL-2			023				
	CHANNEL-3			024				
	CHANNEL-4			025				
	100NS			026				

Fig. 3. Test 13 Data: Load = R3, MOSFET = Q1, Shunt = R2, TEK columns = filenames of CSV files and PNG files respectively

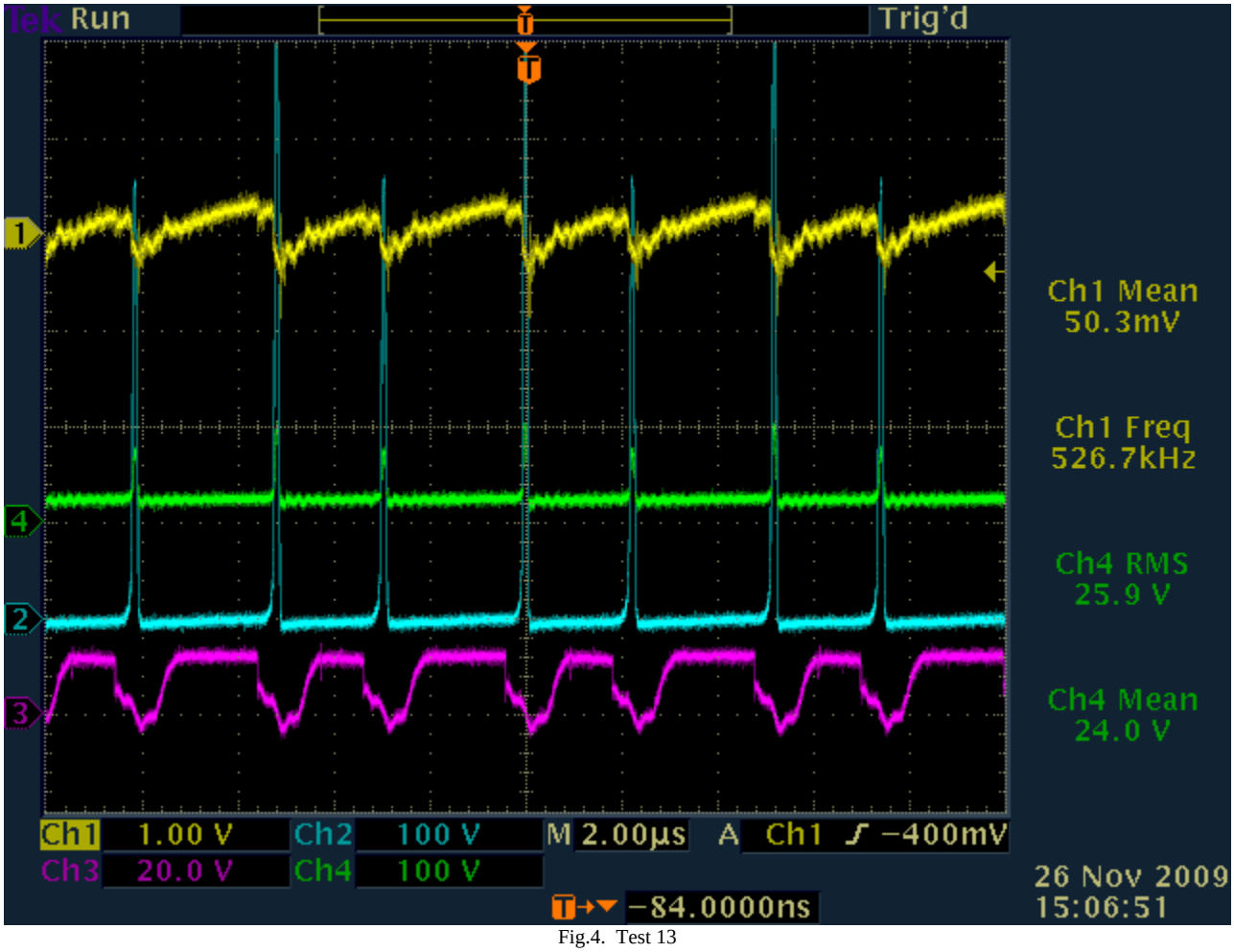
Tek Run
Trig'd
Ch1 Mean
50.3mV
Ch1 Freq
526.7kHz
Ch4 RMS
25.9 V
Ch4 Mean
24.0 V
Ch1 1.00 V
Ch2 100 V
M 2.00µs
A Ch1 −400mV
Ch3 20.0 V
Ch4 100 V
−84.0000ns
26 Nov 2009
15:06:51

Fig.4. Test 13

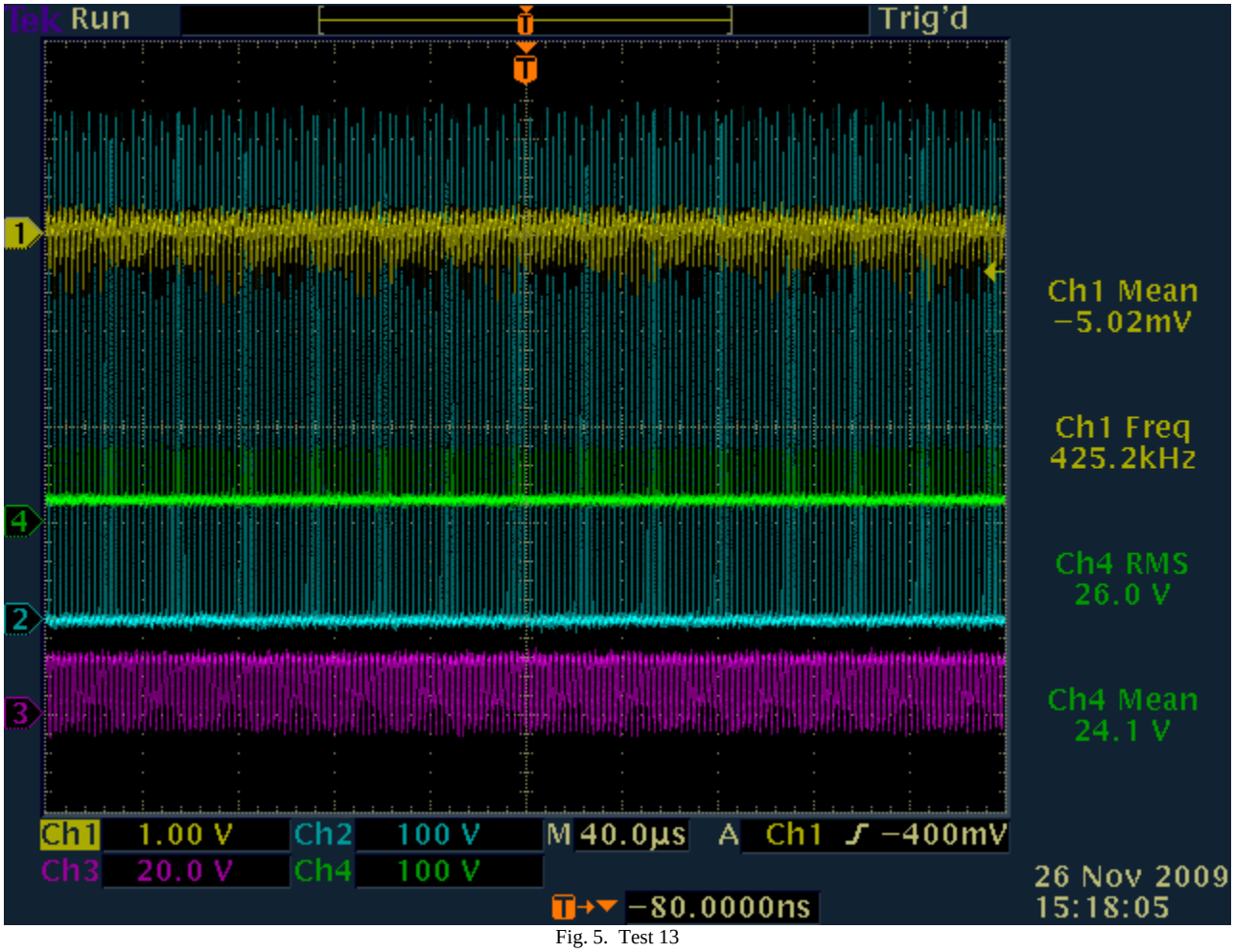
Tek Run
Trig'd
Ch1 Mean
−5.02mV
Ch1 Freq
425.2kHz
Ch4 RMS
26.0 V
Ch4 Mean
24.1 V
Ch1 1.00 V
Ch2 100 V
M 40.0µs
A Ch1 −400mV
Ch3 20.0 V
Ch4 100 V
−80.0000ns
26 Nov 2009
15:18:05

Fig. 5. Test 13

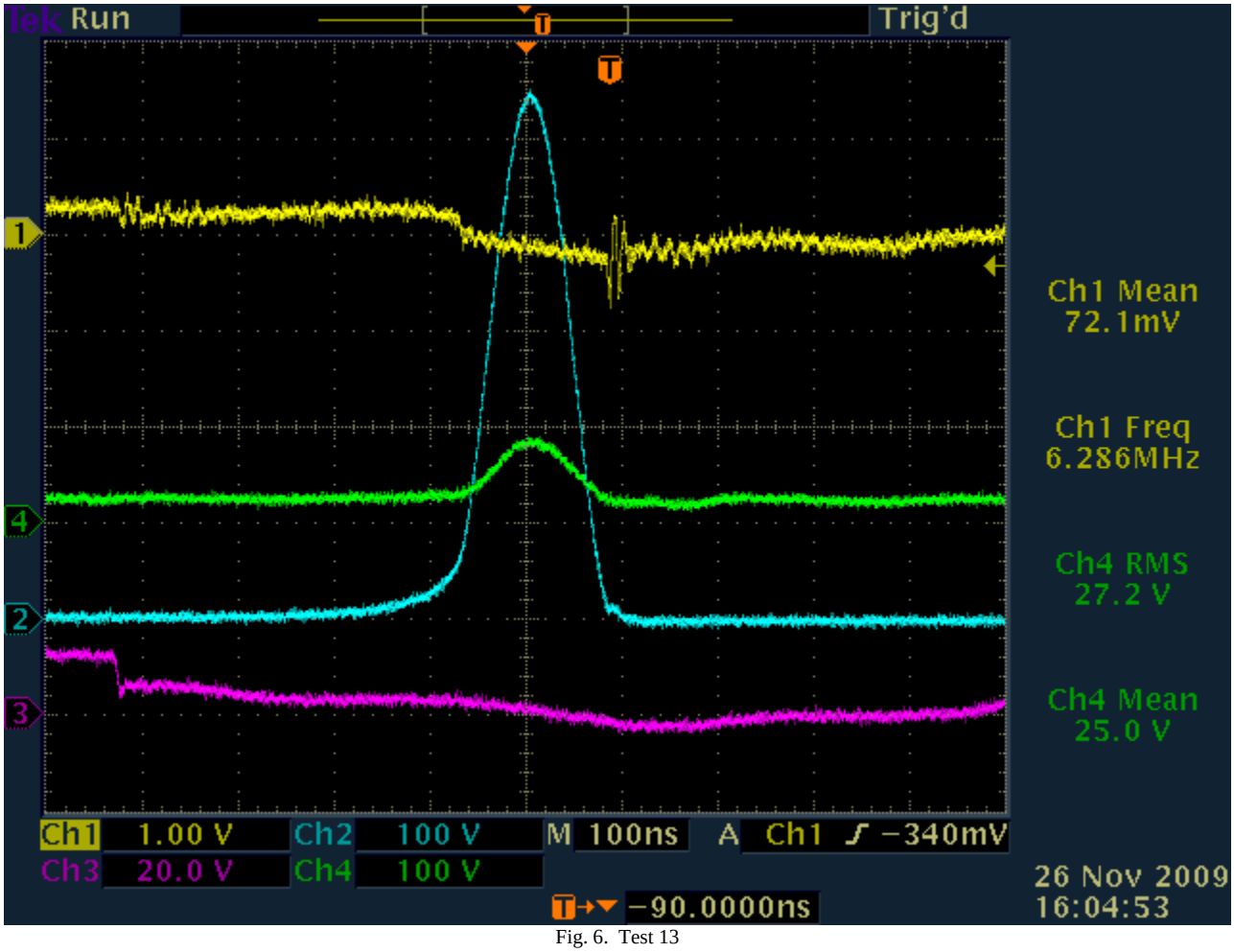
Tek Run
Trig'd
Ch1 Mean
72.1mV
Ch1 Freq
6.286MHz
Ch4 RMS
27.2 V
Ch4 Mean
25.0 V
Ch1 1.00 V
Ch2 100 V
M 100ns
A Ch1 −340mV
Ch3 20.0 V
Ch4 100 V
−90.0000ns
26 Nov 2009
16:04:53

Fig. 6. Test 13